Electronic Supplementary Material (ESI) for Journal of Materials Chemistry A.
This journal is © The Royal Society of Chemistry 2015

Electronic Supplementary Information (ESI)

Supporting Information for

In Situ Preparation of Interconnected Networks Constructed by Flexible Graphene/Sn Sandwich Nanosheets for High-Performance Lithium-Ion Battery Anode

Jian Qin [a], Xiang Zhang [a], Naiqin Zhao [a, b], Chunsheng Shi [a], En-Zuo Liu [a], Jiajun Li [a], and Chunnian He *[, a, b]

[a] *School of Materials Science and Engineering and Tianjin Key Laboratory of Composites and Functional Materials, Tianjin University, Tianjin +86 300072, China*

[b] *Collaborative Innovation Center of Chemical Science and Engineering, Tianjin 300072, China*

* Corresponding author.

E-mail addresses: cnhe08@tju.edu.cn (C. He)

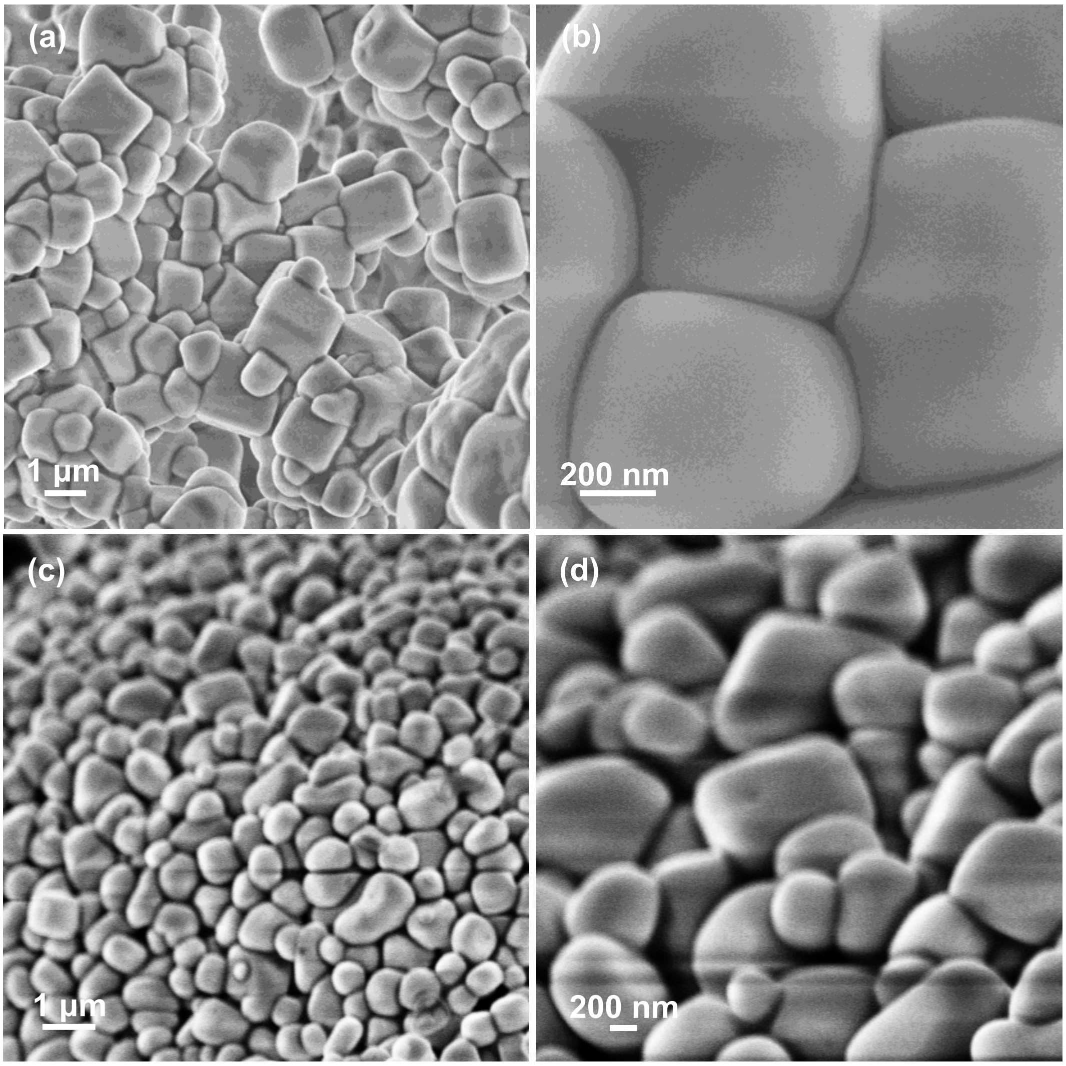

Figure S1. (a) and (b) SEM images of the complex of $SnCl_2$-$C_6H_8O_7$/NaCl after freeze-drying process, suggesting that the NaCl particles uniformly coated with a thin layer of $SnCl_2$-$C_6H_8O_7$ complex were self-assembled into 3D structure during the freeze-drying process. (c) and (d) SEM images of the C-SnO_2 products before eliminating the NaCl, showing that the 3D self-assembly was well preserved after low-temperature calcination of the 3D $SnCl_2$-$C_6H_8O_7$/NaCl and the 3D C-SnO_2 were actually formed on the surface of 3D NaCl self-assembly.

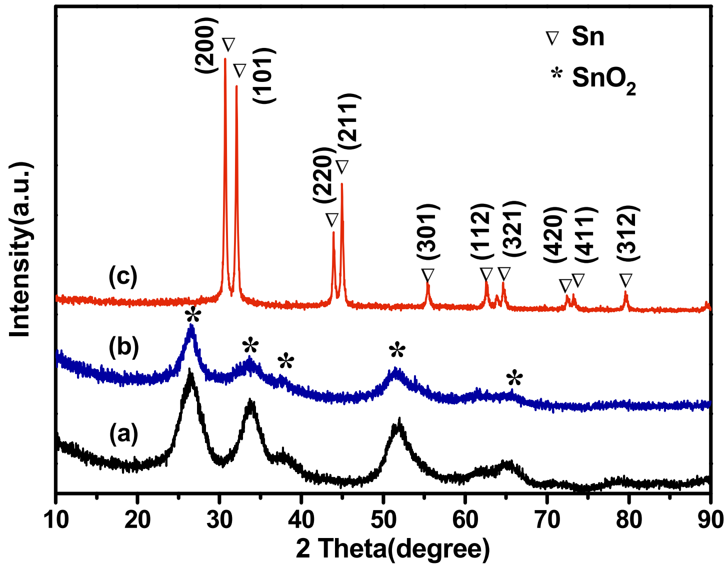

Figure S2. XRD patterns of (a) 3D $SnO_2/C/SnO_2$, (b) 3D $SnO_2/C/SnO_2@C$, and (c) 3D G/Sn/G networks.

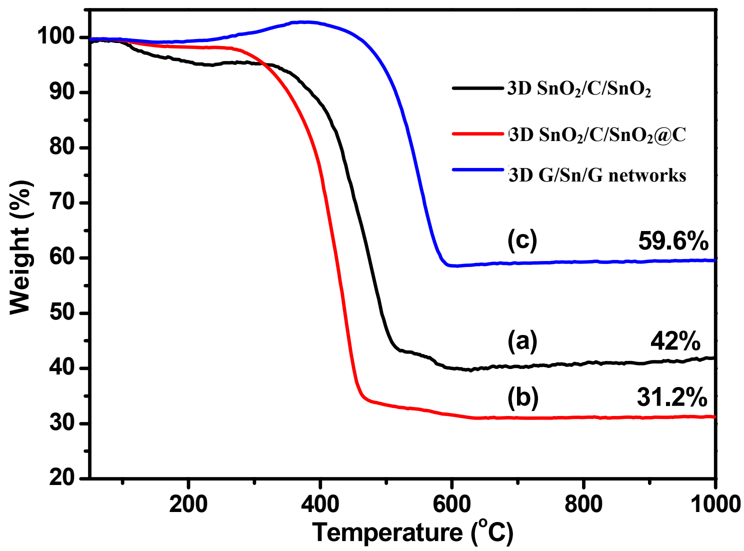

Figure S3. TGA of 3D $SnO_2/C/SnO_2$, 3D $SnO_2/C/SnO_2@C$, and 3D G/Sn/G networks. The Sn contents in the 3D G/Sn/G networks estimated from the thermal analysis are ca. 46.9 wt%. (The sample is annealed under air to oxidize Sn to SnO_2 and carbon to CO_2. On the basis of the final weight of SnO_2, the original content of Sn is calculated to be 46.9 wt %.) Comparing the weight loss of 3D $SnO_2/C/SnO_2$ with that of 3D $SnO_2/C/SnO_2@C$, it can be calculated that approximately 10.8 wt% carbon is added during the hydrothermal process.

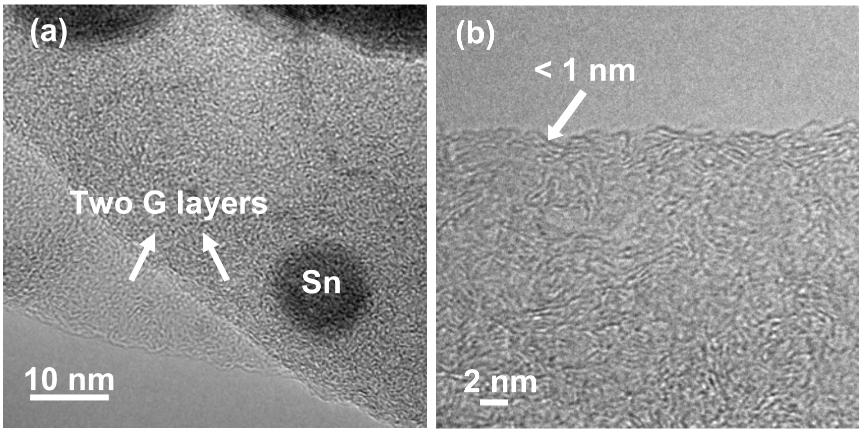

Figure S4. HRTEM images of 3D G/Sn/G networks.

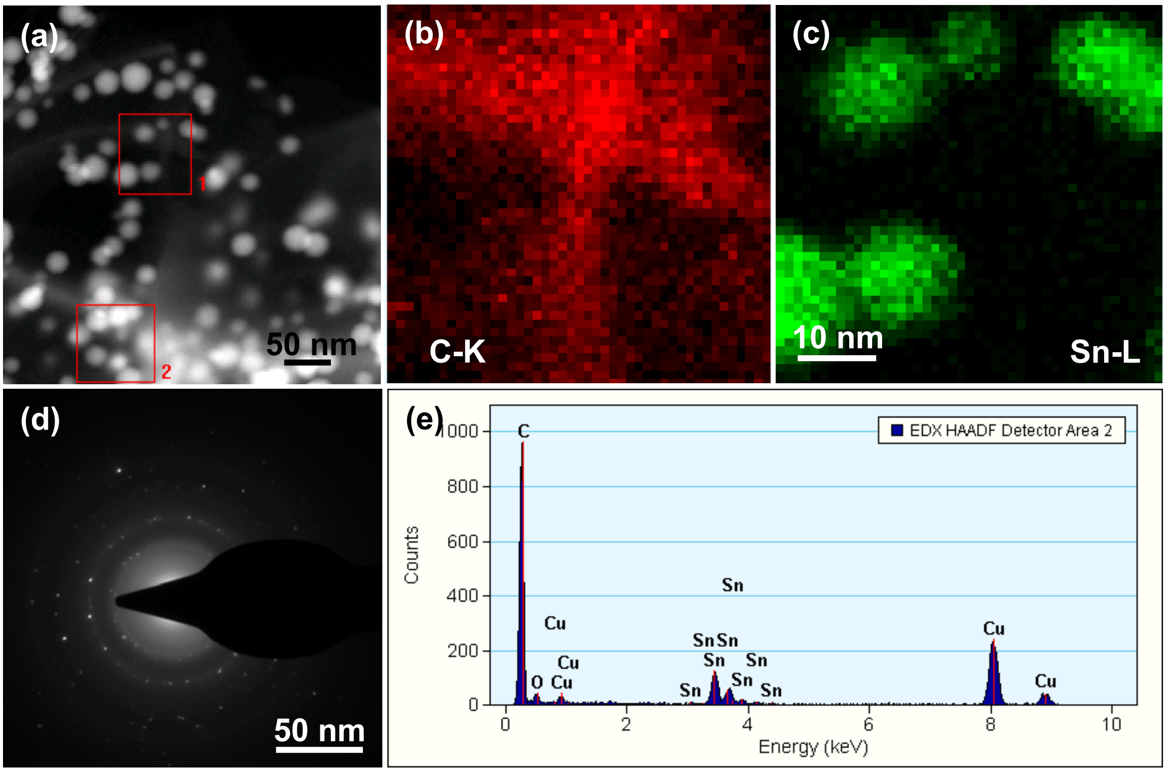

Figure S5. (a) STEM image of 3D G/Sn/G networks. (b) Carbon and (c) Sn element mapping images from area 1 in (a). d) SAED pattern of a typical Sn nanoparticle. e) EDX pattern from area 2 in (a).

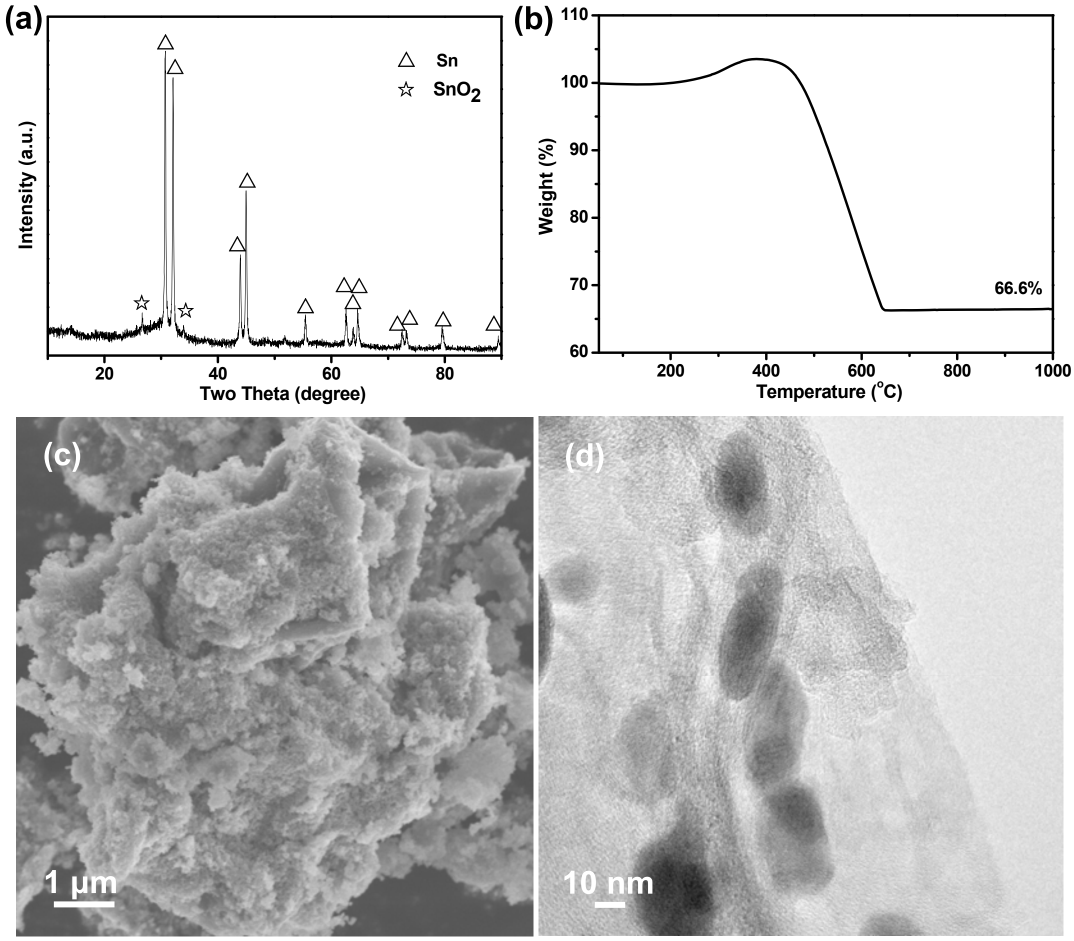

Figure S6. (a) XRD pattern and (b) TGA of G/Sn sandwich nanosheets, showing that the Sn content is about 52 wt.%. (c) SEM and (d) TEM images of G/Sn sandwich nanosheets, indicating a sandwich-like structure with graphene layers closely binding to both sides of metallic Sn nanoparticles or nanosheets.

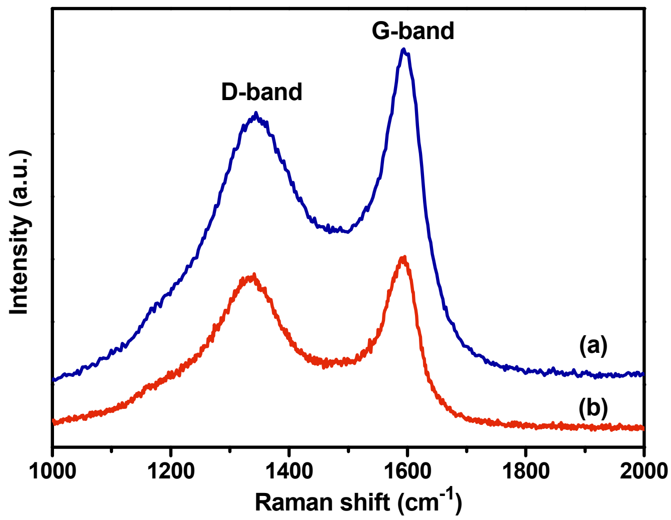

Figure S7. Raman spectra of (a) 3D G/Sn/G networks and (b) G/Sn sandwich nanosheets.

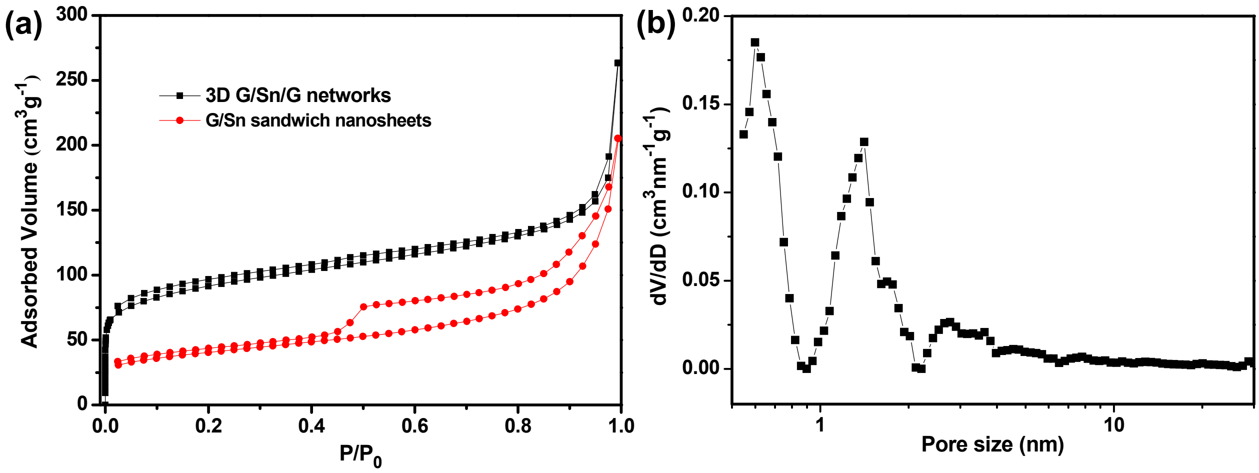

Figure S8. (a) Nitrogen adsorption–desorption isotherms of 3D G/Sn/G networks and G/Sn sandwich nanosheets, and (b) pore size distribution curve of 3D G/Sn/G networks.

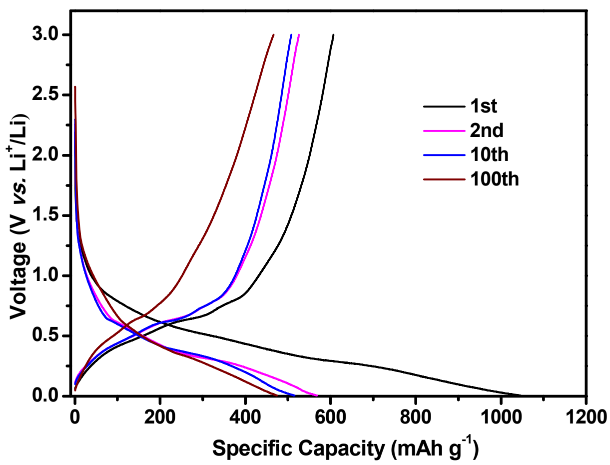

Figure S9. Galvanostatic discharge-charge profiles of G/Sn sandwich nanosheets at a current density of 0.2 A g^{-1}.

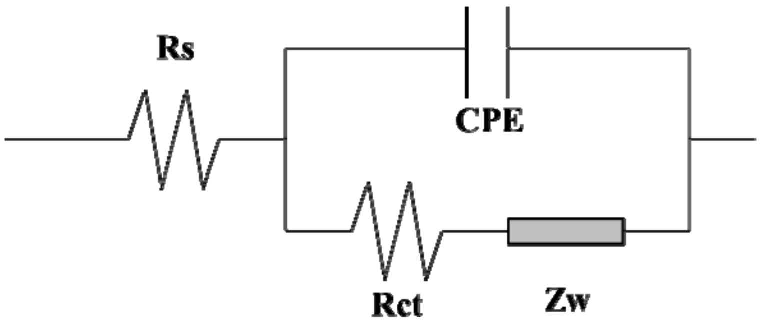

Figure S10. Randles equivalent circuit for 3D G/Sn/G and G/Sn electrode/electrolyte interface. R_s is the electrolyte resistance and the resistance of the surface film formed on the electrodes. R_{ct} is charge-transfer resistance, Z_w is the Warburg impedance related to the diffusion of lithium ions into the bulk electrodes and CPE represents the constant phase element.

Table S1. Comparison of rate performance of 3D G/Sn/G networks electrode with G/Sn sandwich nanosheets electrode on the basis of Figure 4d.

Step number	Number of cycle	Charge/discharge rate (C, 1C = 1 A g^{-1})	Average reversible capacity of 3D G/Sn/G networks electrode (mAh g^{-1})	Average reversible capacity of G/Sn sandwich nanosheets electrode (mAh g^{-1})
1	20	0.2	1011	535
2	40	0.5	871	452
3	60	1	757	385
4	80	2	695	285
5	100	5	438	123
6	120	10	241	64
7	140	0.2	1098	541

Table S2. Comparison of specific capacity and capacity retention at different rates for 3D G/Sn/G networks electrode with those of graphene/Sn sandwich nanosheets, surface-decorated graphene/Sn composites, and various Sn/C composites anodes reported.

Materials	Voltage range (V)	Current density (A g^{-1})	Cycle number	Specific capacity (mAh g^{-1})	Capacity retention (%)
3D G/Sn/G networks [this work]	0.005–3.0	2	500	665	95.5
		0.2	100	1010	97
Graphene/Sn sandwich nanosheets [S1]	0.005–2.0	0.05	60	590	69
Graphene/Sn sandwich nanosheets [S2]	0.002–3.0	1	30	501	86
Graphene/Sn sandwich nanosheets [S21]	0.01–3.0	0.5	100	684.5	76
		1	100	639.7	71
		2	100	552.3	65
		5	100	359.7	51
graphene/Sn composite [S16]	0.005–2.5	0.2	50	255	20
graphene/Sn composite [S17]	0.01–3.0	0.05	30	490	55
graphene/Sn composite [S19]	0.01–3.0	0.5	200	552	87

graphene/Sn composite [S20]	0.02–1.2	0.1	100	500	80
Sn@CNT/graphene composite [S3]	0.005–3.0	2	100	560	82
		1	100	650	78.5
Sn@C/graphene composite [S4]	0.005–2.5	0.05	50	630	70
Sn@C/graphene composite [S12]	0.01–3.0	0.75	100	566	53
Sn/C composite [S6]	0.02–3.0	0.2	130	680	94
Sn/C composite [S7]	0.02−3.0	0.025	300	638	93
Sn/C composite [S15]	0.01–1.5	0.1	100	450	93
Sn/C composite [S18]	0.01–3.0	0.2	200	722	92
Sn@C@carbon fiber [S8]	0.01–3.0	0.25	200	737	88
Sn@mesoporous carbon nanowires [S9]	0.005–2.0	0.1	50	710	57
Sn@mesoporous carbon [S10]	0.005–2.0	0.05	100	560	86
Sn@carbon nanotubes [S11]	0.01–2.5	0.1	100	437	36
Sn@carbon nanotubes [S13]	0.01–2.5	1	100	335	62
Sn@C nanowires [S14]	0.005–2.0	0.1	100	525	55
		0.5	100	490	44
		1	100	486	39
		3	100	286	32
Tin-carbon/silica composite [S5]	0.0–2.5	0.3	100	440	95
Sn@CNT composite [S22]	0.005-3	0.1	80	473.9	90.1
SnQDs@N-CNF composite [S23]	0.02-3	0.2	500	685	74
		0.4	200	508	67
Sn-Co-CNT composite[S24]	0.005-3	0.099	200	811	91.1
		0.99	200	612	85.7
TiO_2 -Sn/C nanowire[S25]	0.01-3	0.335	160	459	99.9
		3.35	100	150	84.8
SnNPs @CNTs composite [S26]	0.005-2	0.1	140	648	83.7
SnNPs@h-CS composite[S27]	0.005-3	0.166	100	550	68.75
Sn NP/CNF hybrid network	0.01-3	0.2	200	460	57.93

composite[S28]					
Sn-PCNF composite[S29]	0.01-3	0.8	200	774	93
RGO/Sn composite[S30]	0.01-2	0.099	50	858	97
Sn/graphene nanocomposite[S31]	0.01-3	0.055	100	508	63.9

Table S3. Kinetic parameters of the electrodes of 3D G/Sn/G networks and G/Sn sandwich nanosheets after the rate capability test.

Samples	$\boldsymbol{R_f}$ **(Ω)**	$\boldsymbol{R_{ct}}$ **(Ω)**
3D G/Sn/G	27.79	66.03
G/Sn	34.91	141.7

References

[S1] B. Luo, B. Wang, X. L. Li, Y. Y. Jia, M. H. Liang, L. J. Zhi, *Adv. Mater.*, 2012, **24**, 3538–3543.

[S2] L. Ji, Z. Tan, T. Kuykendall, E. J. An, Y. Fu, V. Battaglia, Y. Zhang, *Energy Environ. Sci.*, 2011, **4**, 3611–3616.

[S3] Y. Zou, Y. Wang, *ACS Nano*, 2011, **5**, 8108–8114.

[S4] B. Luo, B. Wang, M. H. Liang, J. Ning, X. L. Li, L. J. Zhi, *Adv. Mater.*, 2012, **24**, 1405–1409.

[S5] J. K. Hwang, S. H. Woo, J. M. Shim, C. S. Jo, K. T. Lee, J. Lee, *ACS Nano*, 2013, **7**, 1036–1044.

[S6] Y. H. Xu, Q. Liu, Y. J. Zhu, Y. H. Liu, A. Langrock, M. R. Zachariah, C. S. Wang, *Nano Lett.*, 2013, **13**, 470–474.

[S7] X. F. Li, A. Dhanabalan, L. Gu, C. L. Wang, *Adv. Energy Mater.*, 2012, **2**, 238–244.

[S8] Y. Yu, L. Gu, C. Wang, A. Dhanabalan, P.A. Van Aken, J. Maier, *Angew. Chem. Int. Ed.*, 2009, **48**, 6485–6489.

[S9] Y. C. Qiu, K. Y. Yan, S. H. Yang, *Chem. Commun*., 2010, **46**, 8359.

[S10] Y. G. Wang, B. Li, C. L. Zhang, H. Tao, S. F. Kang, S. Jiang, X. Li, *J. Power Sources*, 2012, **219**, 89.

[S11] X. Y. Hou, H. Jiang, Y. J. Hu, Y. F. Li, J. C. Huo, C. Z. Li, *ACS Appl. Mater. Interfaces*, 2013, **5**, 6672.

[S12] D. N. Wang, X. F. Li, J. L. Yang, J. J. Wang, D. S. Geng, R. Y. Li, M. Cai, T. K. Sham, X. L. Sun, *Phys. Chem. Chem. Phys*., 2013, **15**, 3535.

[S13] H. K. Zhang, H. H. Song, X. H. Chen, J. S. Zhou, *J. Phys. Chem. C*, 2012, **116**, 22774.

[S14] K. C. Hsu, C. E. Liu, P. C. Chen, C. Y. Lee, H. T. Chiu, *J. Mater. Chem*., 2012, **22**, 21533.

[S15] J. Hassoun, G. Derrien, S. Panero, B. Scrosati, *Adv. Mater*., 2008, **20**, 3169.

[S16] Z. H. Wen, S. M. Cui, H. J. Kim, S. Mao, K. H. Yu, G. H. Lu, H. H. Pu, O. Mao, J. H. Chen, *J. Mater. Chem*., 2012, **22**, 3300.

[S17] W. B. Yue, S. Yang, Y. Ren, X. J. Yang, *Electrochim. Acta*, 2013, **92**, 412.

[S18] Z. Q. Zhu, S. W. Wang, J. Du, Q. Jin, T. R. Zhang, F. Y. Cheng, J. Chen, *Nano Lett*., 2014, **14**, 153.

[S19] J. S. Zhu, D. L. Wang, L. B. Cao, T.F. Liu, *J. Mater. Chem. A*, 2014, **2**, 12918.

[S20] F. R. Beck, R. Epur, D. Hong, A. Manivannan, P.N. Kumta, *Electrochim. Acta*, 2014, **127**, 299.

[S21] X. Y. Zhou, Y. L. Zou, J. Yang, *J. Power Sources*, 2014, **253**, 287-295.

[S22] Y. Wang, M. Wu, Z. Jiao, J. Y. Lee, *Chem. Mater*., 2009, **21**, 3210–3215.

[S23] G. H. Zhang, J. Zhu, W. Zeng, S. C. Hou, F. L. Gong, F. Li, C. C. Li, H. G. Duan, *Nano Energy*, 2014, **9**, 61–70.

[S24] Y. Gu, F. D. Wu, Y. Wang, *Adv. Funct. Mater*., 2013, **23**, 893–899.

[S25] J. Y. Liao, A. Manthiram, *Adv. Energy Mater*., 2014, **4**, 1400403.

[S26] Y. Yu, L. Gu, C. Zhu, P.A. Van Aken, J. Maier, *J. Am. Chem. Soc.*, 2009, **131**, 15984–15985.

[S27] W. M. Zhang, J. S. Hu, Y. G. Guo, S. F. Zheng, L. S. Zhong, W. G. Song, L. J. Wan, *Adv. Mater.*, 2008, **20**, 1160–1165.

[S28] J. Wang, W. L. Song, Z. Y. Wang, L. Z. Fan, Y. F. Zhang, *Electrochim. Acta*, 2015, **153**, 468–475.

[S29] Z. Shen, Y. Hu, Y. L. Chen, X. W. Zhang, K. H. Wang, R. Z. Chen, *J. Power Sources*, 2015, **278**, 660-667.

[S30] C. Nithya, S. Gopukumar, *CHEMSUSCHEM*, 2013, **6**, 898–904.

[S31] G. X. Wang, B. Wang, X. H. Wang, J. Park, S. X. Dou, H. Ahn, K. Kim, *J. Mater. Chem.*, 2009, **19**, 8378–8384.